

An Image Forgery Detection Solution based on DCT Coefficient Analysis

Hoai Phuong Nguyen¹, Florent Retraint², Frédéric Morain-Nicolier¹ and Agnès Delahaies¹

¹*CRESTIC, University of Reims Champagne-Ardenne, Reims, France*

²*LM2S, Institute Charles-Delaunay, Troyes University of Technology, Troyes, France*

Keywords: Image Forgery Detection, JPEG Compression, Double Compression, DCT Coefficient.

Abstract: JPEG compression and double JPEG compression introduces systematically some particular characteristics in the Discrete Cosine Transform (DCT) domain. In this paper, we propose a description of these characteristics. We also describe how to exploit these characteristics to introduce a new and efficient solution for estimating the quantization steps used in the first compression of a double-compressed image. We also introduce a method for detecting forgery in compressed images. Rapid, having a simple implementation and there is no need for training to be functional, the proposed solution gives, however, a performance auspicious. Its performance is demonstrated on simulated images and images retrieved from several public databases.

1 INTRODUCTION

With the advent of digital imaging, digital images become an accessible and indispensable source of information. However, due to the availability of several powerful image processing and editing software programs, these images are quite easy to manipulate. In fact, it is possible to add or remove essential contents from an image without exposing any visible traces of tampering. In some case, when the integrity and genuineness of information transmitted are crucial, especially when we use images as critical evidence, it is vital to look for ways to detect and localize forged regions in digital images. There are many techniques to create forged images such as removing objects or regions of images, splicing objects from one image to another, duplicating objects in the same image, etc. These techniques modify locally the information transmitted by the image. They also create some discrepancies between the forged and original region the image. By identifying and highlighting these discrepancies, many forgeries detection solutions have been proposed in the literature.

Forged regions are often scaled, rotated or modified to be coherent to the neighboring unforgered area, which causes the resampling of the local region. The local presence of a resampling operation may be used as evidence of image manipulation. Many resampling detection solutions have been proposed (Popescu and Farid, 2005; Gallagher and Chen, 2008; Mahdian and Saic, 2008; Bunk et al., 2017; Mohammed et al.,

2018). Noise inconsistencies (Mahdian and Saic, 2009; Liu et al., 2014; Yang et al., 2016), lighting artifacts (D and C, 2015) have been also exploited for forgery detection.

Several other solutions exploited different artifacts caused by the JPEG compression process to detect image forgeries. Farid (Farid, 2009) proposed to re-save image under different JPEG qualities then detecting spatially localized local minima in the difference between the image and its JPEG-recompressed counterparts. In many cases, these minima are highly salient and can be detected. Yang et al. (Yang et al., 2014) proposed a method for detecting double JPEG compression with the same quantization matrix, which can be useful for image forgery detection. Bianchi and Piva (Bianchi and Piva, 2012) proposed a image forgery localization method via block-grained Analysis of JPEG Artifacts. The authors in (Ting and Rangding, 2009; Ye et al., 2007; Lin et al., 2009; Wang et al., 2014) proposed to exploit the consistency in the distribution of quantized DCT coefficients to detect and localize tampered regions.

JPEG is a widely used image format which is appropriate for storage and transmission purposes. Distortions caused by JPEG compression can help forgers to better hide their manipulations by disrupting several useful image regularities, such as noise, aberrations, etc. Therefore, the workflow of a digital image forgery often finishes by intentionally or unintentionally resaving the forged image under the JPEG format. If the original image is already in

JPEG format, the final forged image would contain regions where a double compression has been occurred. JPEG compression introduces some particular properties systematically in the DCT domain.

The rest of the paper is organized as follows. Section 2 gives a description of these properties under different situations where a single or a double JPEG compression has been occurred. We introduce after that, in Section 3 a histogram-based solution for the estimation of the first quantization step employed in a double-compressed image. In Section 4, we introduce a new and simple solution for image forgery detection based on the estimation of the first quantization step. The proposed solution has been tested on simulated data and images from some public databases. Experimental results show a good performance of the proposed solution for detecting forged images compressed under high quality factor.

2 SIGNATURE OF JPEG COMPRESSION IN THE DCT DOMAIN

2.1 JPEG Compression

After optionally applying the color space conversion and down sampling, JPEG compression process continues by dividing each color channels into non-overlapped 8×8 blocks. Each block is first transformed in DCT domain. The DCT coefficients of each block will be converted into entire numbers and then quantized.

For a given 8×8 blocks of non-compressed image, let $m_i, i \in \{1, 2, \dots, 64\}$ denote the i -th coefficient obtained after applying DCT on the block. Each coefficient is related to the contribution of an associated frequency in the block. The quantization operation is performed to reduce information in high frequency components, which are often less sensitive to the human visual system. Let $q_i, i \in \{1, 2, \dots, 64\}$ denote the quantization steps employed for quantizing the 64 corresponding DCT coefficients. The value of q_i is constant over all the blocks. It is defined *a priori* in function of the expected Quality Factor. The Quantization Table, constituted by $q_i, i \in \{1, 2, \dots, 64\}$, is stocked as metadata of the JPEG file, which can be easily retrieved during the decompression process.

For a given DCT coefficient, by omitting its index for the sake of simplicity, denote m, c, Q respectively the DCT coefficient, its quantized value and the cor-

responding quantization step. We have that:

$$c = \left\lfloor \frac{m}{Q} \right\rfloor. \quad (1)$$

The JPEG decompression is processed by applying dequantization operation and then the DCT inverse transforms to come back in spatial domain. The dequantized DCT coefficient, denoted d , is obtained by multiplying its corresponding quantized value with the same quantization step used during compression process. We have that:

$$d = cQ = \left\lfloor \frac{m}{Q} \right\rfloor Q. \quad (2)$$

Therefore, the dequantized DCT coefficients are multiples of the corresponding quantization steps.

2.2 JPEG Double Compression

The JPEG double compression involves two successive JPEG compression processes. Figure 1 illustrates different operations occurring in a JPEG double compression. White rectangles represent the different input/output images. Knowing that JPEG compression is processed independently between different 8×8 non-overlapped blocks, we use color rectangles to represent different stages of a block: blue for the first compression and green for the second one. Dashed lines designate the passage between blocks and images. The color space conversion requires blocks from all color channels to process.

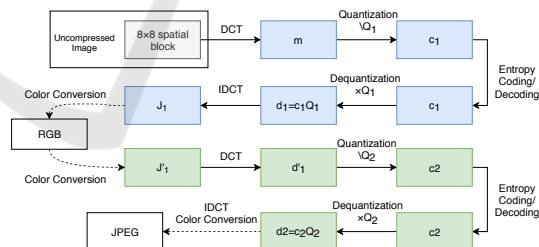


Figure 1: Different operations occurring in a JPEG double compression process. The index of DCT channels is omitted for the sake of simplicity.

For a given DCT frequency, denote $Q_i, c_i, d_i, i \in \{1, 2\}$ respectively the quantization step, the quantized and dequantized DCT coefficient of the i -th compression. Denote d'_1 the DCT coefficient obtained after the second DCT transform. Denote respectively J_1, J'_1 the 8×8 spatial blocks obtained right after the first IDCT transform and before the second DCT transform. Due to rounding error of the color space conversion operations, J'_1 may differ from J_1 . We have that:

$$J' = J + \mathfrak{R}_{CSC}, \quad (3)$$

where \mathfrak{R}_{CSC} is the cumulative errors of the two color space conversion processes. Noting that DCT and IDCT are linear operations, we obtain the following development:

$$\begin{aligned} d'_1 &= \text{DCT}(J'_1) = \text{DCT}(J_1 + \mathfrak{R}_{CSC}) \\ &= \text{DCT}([\text{IDCT}(d_1)] + \mathfrak{R}_{CSC}) \\ &= \text{DCT}(\text{IDCT}(d_1) + \mathfrak{R} + \mathfrak{R}_{CSC}) \\ &= d_1 + \mathfrak{E} = c_1 Q_1 + \mathfrak{E}, \end{aligned} \quad (4)$$

where $\mathfrak{E} = \text{DCT}(\mathfrak{R} + \mathfrak{R}_{CSC})$, \mathfrak{R} is the rounding error of the IDCT transform, and $[\cdot]$ is the round-off function. \mathfrak{E} can be considered as random variable centered at 0, with a high probability of dropping in the $] -1, 1[$ interval ($> 90\%$), (Thai et al., 2017). Finally, we obtain the following equation of c_2 :

$$c_2 = \left\lfloor \frac{c_1 Q_1 + \mathfrak{E}}{Q_2} \right\rfloor. \quad (5)$$

3 QUANTIZATION STEP ESTIMATION

Given a JPEG image, we can retrieve the quantized DCT coefficients easily and the Quantization Table from JPEG file. However, in double-compressed images, the quantization step and the exact values of quantized DCT coefficients involved in the first compression would be lost after the second one. For forensics purposes, it is proposed to estimate the lost Q_1 knowing Q_2 and having a sample of c_2 . Lou et al. (Luo et al., 2010), Thai et al. (Thai et al., 2017) have proposed different solutions for estimating quantization step from an image that has been previously JPEG-compressed and then stored in lossless format. These solutions solve only a particular case of the proposed problem, when $Q_2 = 1$. Pevny and Fridirich (Pevny and Fridirich, 2008) have proposed a method for the detection of double JPEG compression using a soft-margin support vector machine. The 144-dimensional features vector employed contains the number of occurrences of the first 16 multiples of the second quantization step retrieved from the first 9 AC frequencies. They have also proposed a multiclassifier which permits detecting Q_1 for the first 9 AC frequencies when $Q_2 \in \{4, 5, 6, 7, 8\}$.

In this section, we propose a new histogram-based approach for the estimation of Q_1 knowing Q_2 and having a sample of c_2 . Let consider Equation 14, knowing that \mathfrak{E} is a random variable which drops into the $] -1, 1[$ interval with a very high probability, we have that:

$$\left\lfloor \frac{c_1 Q_1}{Q_2} \right\rfloor - 1 \leq c_2 \leq \left\lfloor \frac{c_1 Q_1}{Q_2} \right\rfloor + 1 \quad (6)$$

and it is more likely that $c_2 = \left\lfloor \frac{c_1 Q_1}{Q_2} \right\rfloor$. It means that the histogram of a sample of c_2 will highly likely contains peaks located at $\left\lfloor \frac{k Q_1}{Q_2} \right\rfloor, k \in \mathbb{Z}$. Furthermore, basing on the statistical model of DCT coefficients proposed by Thai et al (Thai et al., 2013), it is likely that:

$$h\left(\left\lfloor \frac{k_1 Q_1}{Q_2} \right\rfloor\right) > h\left(\left\lfloor \frac{k_2 Q_1}{Q_2} \right\rfloor\right) \quad (7)$$

for $0 \leq k_1 < k_2$ or $0 \geq k_1 > k_2$ where $h(x)$ denotes the number of occurrences of x in the histogram.

Given Q_1 , by varying k , we can predict all the possible values of $\left\lfloor \frac{k Q_1}{Q_2} \right\rfloor$, and then all the possible peaks of the histogram. Denote $\mathbf{P}_{Q_1} = \{p_i, i \in \mathbf{I}_{P_{Q_1}}\}$, and $\mathbf{H} = \{x_i, i \in \mathbf{I}_H\}$ respectively the sets of predicted peaks' location and actual peaks' location of c_2 sample's histogram, where $\mathbf{I}_{P_{Q_1}}, \mathbf{I}_H$ are respectively the sets of index of \mathbf{P}_{Q_1} and \mathbf{H} , we propose a measure of the difference between the set \mathbf{P}_{Q_1} and the histogram of c_2 sample, denoted by $S(\mathbf{P}_{Q_1}, \mathbf{H})$, as follows:

$$S(\mathbf{P}_{Q_1}, \mathbf{H}) = \sum_{p \in \mathbf{P}_{Q_1}} (f_H(p) - h(p)) + \sum_{p \in \mathbf{H}} (1 - e_{P_{Q_1}}(p)) f_H(p), \quad (8)$$

where

$$e_X(p) = \begin{cases} 1 & \text{if } p \in \mathbf{X} \\ 0 & \text{if } p \notin \mathbf{X} \end{cases} \quad (9)$$

and $f_H(x)$ is the score function, which is empirically defined from the histogram of the c_2 sample as follows:

$$f_H(\varepsilon x_i + (1 - \varepsilon)x_{i+1}) = \varepsilon h(x_i) + (1 - \varepsilon)h(x_{i+1}) \quad (10)$$

for all $\varepsilon \in [0, 1]$ and x_i, x_{i+1} are any two successive elements of \mathbf{H} . In the equation 8, the first term accounts for the difference contributed by DCT values belonging to \mathbf{P}_{Q_1} , the second term accounts for the difference contributed by DCT values belonging to \mathbf{H} but not belonging to \mathbf{P}_{Q_1} . DCT values which do not belong to $\mathbf{H} \cup \mathbf{P}_{Q_1}$ are not taken into account in the proposed measure of difference. Figure 2 shows a typical histogram of DCT coefficients (for a given frequency) knowing that $Q_1 = 15$ and $Q_2 = 2$. The score function $f_H(x)$ is given in red. Figure 3 illustrates different terms contributing in the measure of difference $S(\mathbf{P}_{Q_1}, \mathbf{H})$ where $Q_1 = 15, Q_2 = 2$ and the predicted value of Q_1 is set at 9.

The value of Q_1 which minimizes the measure of difference $S(\mathbf{P}_{Q_1}, \mathbf{H})$ is the best estimation for the unknown Q_1 . Figure 4 illustrates the evolution of the measure of difference $S(\mathbf{P}_{Q_1}, \mathbf{H})$ when Q_1 varies from 1 to 100.

The proposed method for estimation of the first quantization step performs correctly when $Q_1 > Q_2$,

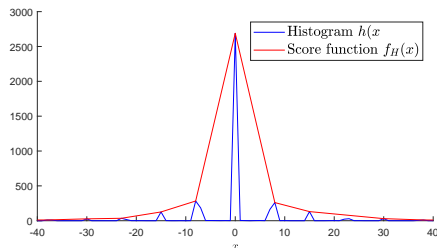


Figure 2: Histogram of DCT coefficients and the proposed scoring function ($Q_1 = 15, Q_2 = 2$).

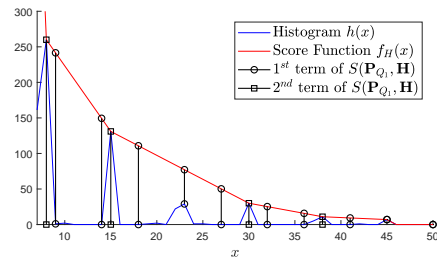


Figure 3: Illustration of different terms contributing in $S(\mathbf{P}_{Q_1}, \mathbf{H})$ where $Q_1 = 15, Q_2 = 2$ and the predicted value of Q_1 is set at 9.

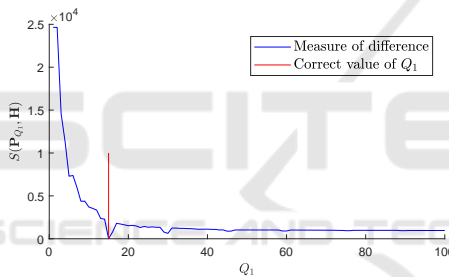


Figure 4: Typical evolution of the measure of difference $S(\mathbf{P}_{Q_1}, \mathbf{H})$ ($Q_1 = 15, Q_2 = 2$).

which means that the Quality Factor (QF) of the second compression must be greater than the QF of the first one. Furthermore, the estimation of Q_1 in high DCT frequencies is not reliable due to insufficient statistics.

4 PROPOSED FORGERY DETECTION SOLUTION

In this study, we only consider the cases where forged images are created by modifying locally an authentic JPEG image, titled here as the carrier image. When a region of the carrier image is forged, because of many reasons, the DCT coefficients within the forged region do not have the same behavior of the ones in the rest of the image. The reasons could be:

- The forged region comes from an uncompressed image or an image compressed using Quantifica-

tion Table different from the one utilized in the carrier image.

- Manipulations such as filtering, interpolating, scaling, etc. during the forgery process break the characteristics of quantized DCT coefficients of the forged region.
- There may be some mismatch of the DCT grid of the forged region with that of the rest of the image. When the forged image is recompressed to save, the forged region is forced to use the same DCT grid as the whole image. Traces of the first compression will disappear for blocks within forged region.

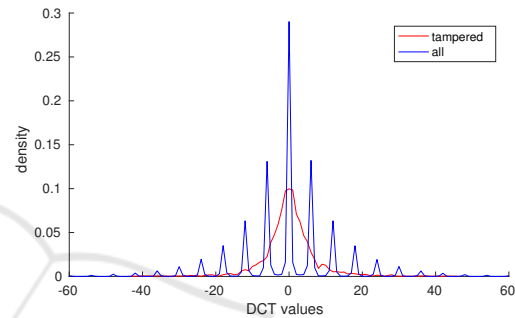


Figure 5: Normalized histograms of DCT coefficients at a given frequency of a forged image (blue curve) and of the forged region within the same image (red curve).

Figure 5 shows the normalized histograms of DCT coefficients at a given frequency of a forged image and of the forged region within the same image. When the area of the forged region is small enough in comparison to the whole image’s area, the DCT coefficients of blocks within the forged region do not contribute much into the shape of the whole image’s DCT histograms. Then, we can employ these DCT histograms, extracted from the whole image, to estimate the quantization steps of the JPEG compression realized previously on the carrier image.

For a given DCT channel, having the corresponding estimated quantization step, we can predict all the values possible of its DCT coefficients, $\mathbf{P} = \{p_i, i \in \mathbf{I}_P\}$. If the estimation is precise, blocks of which the corresponding DCT coefficient do not belong to the set of predicted DCT values can be considered as forged ones. Denote $\mathbf{Z} = \{z_i | i \in \mathbf{I}_B\}$ the set of all DCT values belonging to the channel, where \mathbf{I}_B is the set of 8×8 block indexes. We propose a score map $\mathbf{S} = \{s_i | i \in \mathbf{I}_B\}$ for forgery detection, which is defined as follows:

$$s_i = f_P(z_i), \tag{11}$$

where the score function $f_S(z)$ is defined as follows:

$$f_P(z) = \begin{cases} d_P(z) & \text{if } d_P(z) > 1 \\ 0 & \text{if } d_P(z) \in \{0, 1\} \end{cases} \quad (12)$$

and the function $d_P(z)$ returns the distance from z to the nearest element of \mathbf{P} . For any z , there always exists p and q ($p < q$) two successive elements of \mathbf{P} and $\alpha \in [0, 1)$ such as $z = \alpha p + (1 - \alpha)q$, $d_P(z)$ is defined as follows:

$$d_P(z) = \min(\alpha, 1 - \alpha)(q - p). \quad (13)$$

The score function $f_P(z)$ is set to the distance $d_P(z)$, because we simply consider that the more a DCT value is far from its nearest $p \in \mathbf{P}$, the more likely that it belongs to the forged region. When $d_P(z) \leq 1$, it is highly likely that the related block belongs to forged regions. To minimize the false detection rate, $f_P(z)$ is set to zero in these cases.

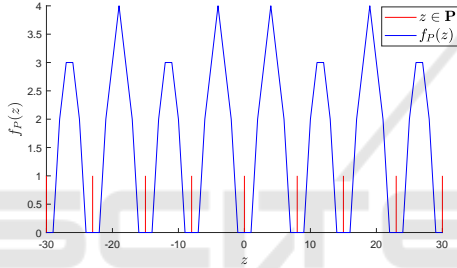


Figure 6: Illustration of the function $f_P(z)$ where the set \mathbb{P} is defined with $Q_1 = 15$ and $Q_2 = 2$.

Hence, for every DCT channels where we can estimate the first quantization step, we can produce a score map. By summing up all these individual score maps, we obtain a global score map, which permits detecting and localizing forgeries. The presence in cluster of non-zero scores in the global score map permits highlighting and localizing forged regions. However, a zero score map cannot provide us sufficient means to confirm the authenticity of an image.

5 NUMERICAL RESULTS

5.1 Estimation of the First Quantization Step

To evaluate the performance of the proposed solution for the estimation of the first quantization step, for each couple of (Q_1, Q_2) $Q_1 \in \{1, 2, \dots, 100\}$ and $Q_2 \in \{1, 2, \dots, 50\}$, we generate a sample of c_2 . The generated sample of c_2 would be used to obtain an estimated value of Q_1 , denoted \hat{Q}_1 . We finally compare \hat{Q}_1 and its correct counterpart Q_1 . The sample

of c_2 contains 4096 elements, which corresponds to the number of 8×8 blocks of a 512×512 image. Each element of the sample is obtained by the following equation:

$$c_2 = \left\lfloor \frac{\left\lceil \frac{m}{Q_1} \right\rceil Q_1 + \mathfrak{E}}{Q_2} \right\rfloor, \quad (14)$$

where m represents a value of a non-quantized DCT coefficient, which is modeled as a sample of a zero-mean Laplacian random variable with the scale parameter $b = 128$, knowing that the probability density function of a zero-mean Laplacian random variable with the scale parameter b is given as follows:

$$f(x) = \frac{1}{2b} \exp\left(-\frac{|x|}{b}\right), \text{ where } x \in \mathbb{R}, \quad (15)$$

and \mathfrak{E} is a zero-mean random variable where

$$P(\mathfrak{E} \in]-1, 1[) = 0.9.$$

Figure 7 shows the values of $|\hat{Q}_1 - Q_1|$ for different values of Q_1 and Q_2 . The proposed algorithm can define precisely in most of the cases when $Q_1 > 2Q_2$. When $Q_2 < 15$, the proposed algorithm can also define precisely some value of Q_1 which is smaller than $2Q_2$ and greater than Q_2 . When $Q_1 = 2Q_2$ or $Q_1 < Q_2$, the proposed algorithm fails to estimate Q_1 . The bigger the value of Q_2 is, the more the performance of the proposed estimation algorithm decreases.

The proposed estimation method relies on the dynamic in value of the c_2 sample. If the distribution of m has a small scale parameter and when Q_1 and Q_2 are big enough, all or most of the value of c_2 sample will be zero. The other values of c_2 , if exist will create one or two small peaks far from the principal peak, which is located at 0. The poor dynamic of the related histogram does not permit to obtain a good estimation using the proposed method. The size of the c_2 sample is also a factor which impacts directly on the performance of the proposed method.

5.2 Forgery Detection Performance on Simulated Images

The proposed forgery detection solution has been first tested on simulated images. We have employed two 512×512 TIFF images (*boats512x512.tif* and *bridges512x512.tif*) for the simulation, Figures 8a and 8b. The *boats* and *bridges* images are respectively used as carrier and donner for a splicing operation. The two images are respectively compressed with a quality factor equal to QF_1 and 95. Assuming that the forger possesses only the compressed version of the two images. The forged image, Figure 8c, is simply

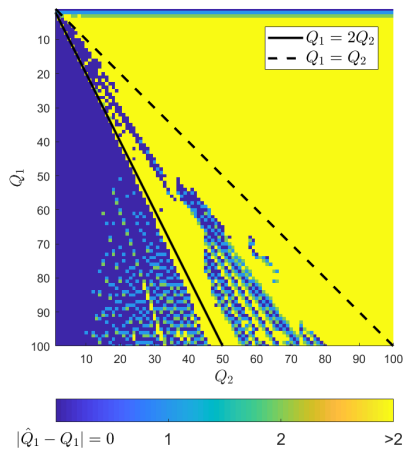


Figure 7: Performance of the proposed method for the estimation of Q_1 for different values of Q_2 visualized via the value of $|\hat{Q}_1 - Q_1|$.

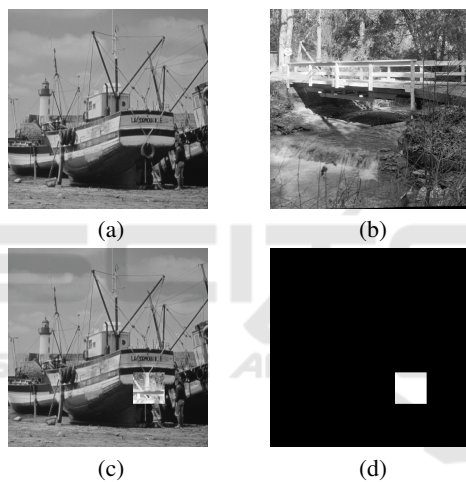


Figure 8: Simulation of splicing forgery: (a) Carrier image *boats512x512.tif*, (b) Donner image *bridges512x512.tif*, (c) forged image created by splicing (d) ground truth.

created by copying a small square of the *bridge's* image and then pasting it on an arbitrary position within the *boat's* image. Figure 8d gives the ground-truth of the given forged image. After the splicing operation, the forger would resave the forged image under the JPEG format, and the QF selected for the JPEG compression is QF_2 .

Quality Factor of a JPEG compression varies from 1 to 100. When $QF = 1$, all the 64 quantization steps will be set to 255, the compressed image lost almost its information. When $QF = 100$, all the 64 quantization steps will be set to 1, there is no compression and the image is in its best quality. For different values of QF_1 and QF_2 varying from 1 to 100, we created a forged image. The proposed method for image forgery detection is then applied on the image to detect the forged region. We evaluated the detection

performance by studying the number of forged block correctly detected and the number of unforged blocks incorrectly classified for different values of QF_1 and QF_2 .

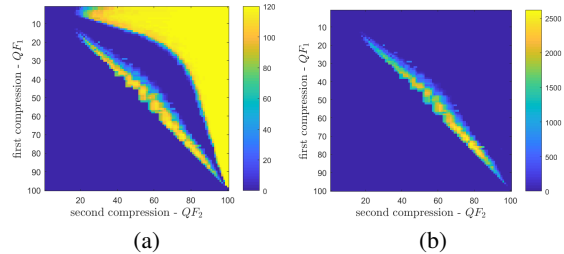


Figure 9: Number forged blocks correctly detected (a) and number of unforged blocks incorrectly classified (b) for different values of Quality Factor of the first and second JPEG compressions. Simulated images contain 4096 8×8 -blocks in total and the number of forged blocks is 120.

Figure 9a and Figure 9b describe respectively the number of forged block correctly detected and the number of unforged blocks incorrectly classified for different values of QF_1 and QF_2 . By comparing the two figures, we can see that the proposed solution performs well over a big set of a couple of (QF_1, QF_2) . For every couple of (QF_1, QF_2) which locates in the yellow region in the top-right corner of Figure 9a, the detection of forged region is precise. For couples which locate on the hot color regions which present on both Figure 9a and Figure 9b, the proposed solution performs badly with a very high number of unforged blocks misclassified. The blue region represents all the couples (QF_1, QF_2) where the forged image can bypass the proposed detection solution.

5.3 Forgery Detection Performance on Images from Public Database

As demonstrated in the previous section, we admit that our method cannot detect all forgeries. It can only detect forgery for JPEG images which were created from JPEG images and resaved with a QF greater than the QF of the original ones. When forged images is resaved under an uncompressed format such as TIFF, we can consider that $Q_2 = 1$ for all the 64 DCT coefficients. We can then obtain an estimated sample of c_2 by applying the DCT manually transform. The proposed solution performs well in these cases. We have tested our image forgery detection solution on the two public databases CASIA v1 and CASA v2 (Dong et al.,). For $QF_2 > 95$, our method performs well for most of the case, we restricted therefore to study images which have QF greater than 95. From the CASIA databases, we have extracted a set of 177 forged images. The proposed solution achieved to lo-

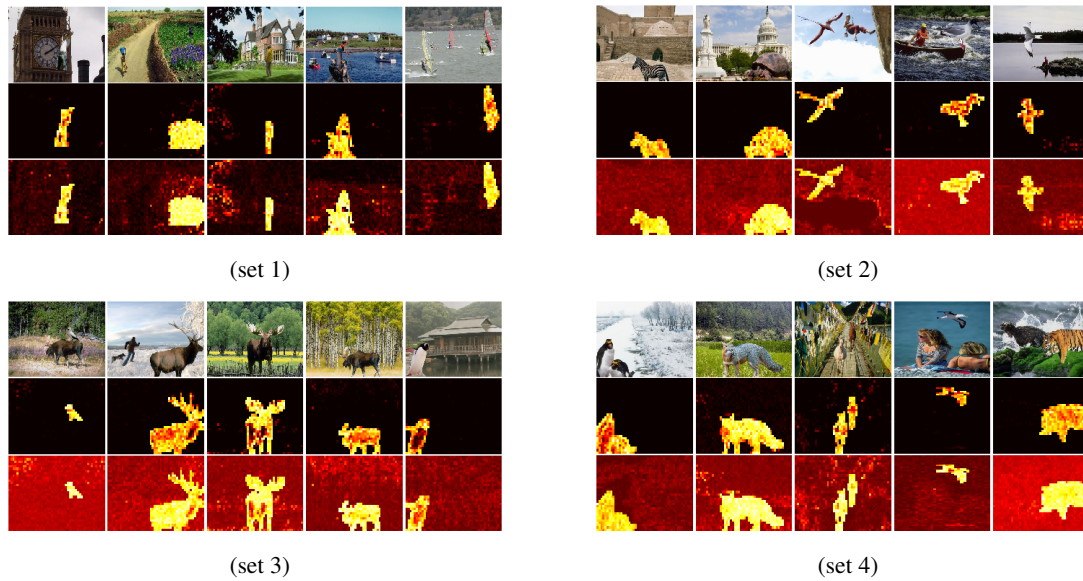


Figure 11: Forged images from CASIA (first row), result maps of the proposed method (middle row), and results given by (Lin et al., 2009) (last row).

calize partially or entirely the forged region in 169 over 177 extracted images.

Figure 11 shows examples where we can detect entirely the forged region of the image. The proposed solution is compared with Lin et al.’s solution (Lin et al., 2009). The proposed solution gives a detection map much less noisy than the one given by (Lin et al., 2009).

Figure 10 shows examples where we can detect only a portion of forged region from the image. Most of undetected forged blocks are situated in homogeneous or saturated regions, where there is not too much information, and they cannot be exposed by the proposed solution, Figure 10a. For some images, forged and unforged regions are previously compressed under the same conditions, and the forged region’s DCT grid matches correctly the one of the rest of the image. Blocks within the forged region of these images are undetected. However, forged the region in general is not created as a set of 8×8 -blocks but as a cluster of pixels. Therefore, blocks situated in the boundaries of forged region can contain some pixels from the unforged one. This spatial combination changes obviously the characteristics of DCT coefficients of these blocks, which makes them exposed under the proposed detection method. When blocks on the boundaries region are detected, the forged region can also be detected and localized, see Figure 10b for example.

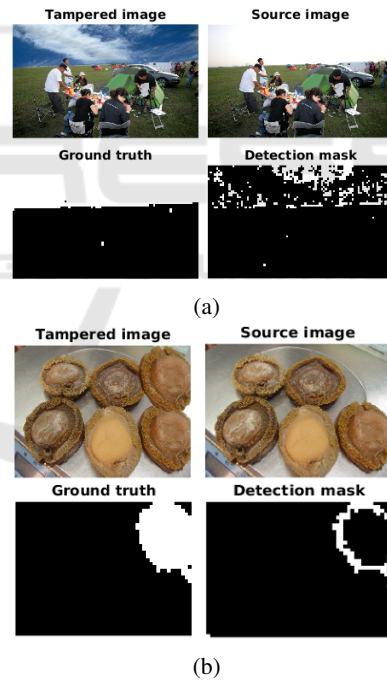


Figure 10: Example of partial detection of forged region.

6 CONCLUSION

In this paper, by analyzing the characteristics of JPEG compression in the DCT domain, we propose a new and efficient histogram-based solution for estimating the quantization steps utilized in the first compression of a double-compressed JPEG image. The pro-

posed solution performs precisely when the quantization step used in the first compression is greater than the double of the one used in the second compression.

We also propose a simple and fast solution for exposing forgeries in compressed images. Given an image, assuming that it is double-compressed, we try to detect the quantization step used in the first compression for all the DCT coefficients. Having the first quantization step, we can create a model for the value of the doubly quantized DCT coefficient. Blocks of which the DCT coefficients do not follow the given model are considered as forged. The proposed solution was tested on both simulated and real images. Forged images created from JPEG images and re-saved under high quality JPEG can be detected correctly, and forged region can be localized precisely with the proposed method.

ACKNOWLEDGEMENT

This work was supported by ANR project DEFACTO ANR-16-DEFA-0002.

REFERENCES

- Bianchi, T. and Piva, A. (2012). Image forgery localization via block-grained analysis of JPEG artifacts. *IEEE Transactions on Information Forensics and Security*, 7(3):1003–1017.
- Bunk, J., Bappy, J. H., Mohammed, T. M., Nataraj, L., Flenner, A., Manjunath, B. S., Chandrasekaran, S., Roy-Chowdhury, A. K., and Peterson, L. (2017). Detection and localization of image forgeries using resampling features and deep learning. *arXiv:1707.00433 [cs]*.
- D, R. P. and C, A. (2015). Image forgery detection using SVM classifier. In *2015 International Conference on Innovations in Information, Embedded and Communication Systems (ICIIECS)*, pages 1–5.
- Dong, J., Wang, W., and Tan, T. CASIA image tampering detection evaluation database. In *2013 IEEE China Summit and International Conference on Signal and Information Processing*, pages 422–426.
- Farid, H. (2009). Exposing digital forgeries from JPEG ghosts. *IEEE Transactions on Information Forensics and Security*, 4(1):154–160.
- Gallagher, A. C. and Chen, T. (2008). Image authentication by detecting traces of demosaicing. In *2008 IEEE Computer Society Conference on Computer Vision and Pattern Recognition Workshops*, pages 1–8.
- Lin, Z., He, J., Tang, X., and Tang, C.-K. (2009). Fast, automatic and fine-grained tampered JPEG image detection via DCT coefficient analysis. *Pattern Recognition*, 42(11):2492–2501.
- Liu, B., Pun, C.-M., and Yuan, X.-C. (2014). Digital image forgery detection using JPEG features and local noise discrepancies. *The Scientific World Journal*, 2014.
- Luo, W., Huang, J., and Qiu, G. (2010). JPEG error analysis and its applications to digital image forensics. *IEEE Transactions on Information Forensics and Security*, 5(3):480–491.
- Mahdian, B. and Saic, S. (2008). Blind authentication using periodic properties of interpolation. *IEEE Transactions on Information Forensics and Security*, 3(3):529–538.
- Mahdian, B. and Saic, S. (2009). Using noise inconsistencies for blind image forensics. *Image and Vision Computing*, 27(10):1497–1503.
- Mohammed, T. M., Bunk, J., Nataraj, L., Bappy, J. H., Flenner, A., Manjunath, B. S., Chandrasekaran, S., Roy-Chowdhury, A. K., and Peterson, L. (2018). Boosting image forgery detection using resampling detection and copy-move analysis. *arXiv:1802.03154 [cs]*.
- Pevny, T. and Fridrich, J. (2008). Detection of double-compression in JPEG images for applications in steganography. *IEEE Transactions on Information Forensics and Security*, 3(2):247–258.
- Popescu, A. C. and Farid, H. (2005). Exposing digital forgeries by detecting traces of resampling. *IEEE Transactions on Signal Processing*, 53(2):758–767.
- Thai, T. H., Cogranne, R., and Reiraint, F. (2013). Steganalysis of jsteg algorithm based on a novel statistical model of quantized DCT coefficients. In *2013 IEEE International Conference on Image Processing*, pages 4427–4431.
- Thai, T. H., Cogranne, R., Reiraint, F., and Doan, T. N. C. (2017). JPEG quantization step estimation and its applications to digital image forensics. *IEEE Transactions on Information Forensics and Security*, 12(1):123–133.
- Ting, Z. and Rangding, W. (2009). Doctored JPEG image detection based on double compression features analysis. In *2009 ISECS International Colloquium on Computing, Communication, Control, and Management*, volume 2, pages 76–80.
- Wang, W., Dong, J., and Tan, T. (2014). Exploring DCT coefficient quantization effects for local tampering detection. *IEEE Transactions on Information Forensics and Security*, 9(10):1653–1666.
- Yang, J., Xie, J., Zhu, G., Kwong, S., and Shi, Y. (2014). An effective method for detecting double JPEG compression with the same quantization matrix. *IEEE Transactions on Information Forensics and Security*, 9(11):1933–1942.
- Yang, Q., Peng, F., Li, J.-T., and Long, M. (2016). Image tamper detection based on noise estimation and lacunarity texture. *Multimedia Tools and Applications*, 75(17):10201–10211.
- Ye, S., Sun, Q., and Chang, E. (2007). Detecting digital image forgeries by measuring inconsistencies of blocking artifact. In *2007 IEEE International Conference on Multimedia and Expo*, pages 12–15.